

Supplementary Information

Multi-functional piezoelectric energy harvesters based on porous PLLA/BaTi₂O₅ piezocomposite films

Yuanbiao Gong,^a Weijia Wang,^{*a} Jiahao Cao,^b Xiaohu Ren,^c Yuxin Jia,^d Yidi Duan,^a Bodong Wang,^a Qinghua Guo,^b Yafei Feng^{*be} and Huiqing Fan^{*a}

^a *State Key Laboratory of Solidification Processing, School of Materials Science and Engineering, Northwestern Polytechnical University, Xi'an 710072, P. R. China*

^b *Department of Orthopedics, Xijing Hospital, The Fourth Military Medical University, Xi'an, 710032, P. R. China*

^c *College of Materials Science and Engineering, Xi'an University of Architecture and Technology, Xi'an 710055, P. R. China*

^d *School of Electronics and Information, Northwestern Polytechnical University, Xi'an 710129, P. R. China*

^e *State Key Laboratory of Oral & Maxillofacial Reconstruction and Regeneration, The Fourth Military Medical University, Xi'an, 710032, P. R. China*

*E-mail addresses of corresponding authors:

E-mail address: weijia.wang@nwpu.edu.cn (W. Wang).

Experimental Section

Raw Materials: Barium carbonate (BaCO_3 , 99.8%), titanium dioxide (TiO_2 , 99%), sodium chloride (NaCl , 99.5%), potassium chloride (KCl , 99.5%), and DXA were purchased from Shanghai Aladdin Biochemical Technology Co., Ltd. (Shanghai, China). Silane coupling agent KH-560 and hydrochloric acid (HCl) were purchased from Sinopharm Chemical Reagent Co., Ltd. (Shanghai, China). PLLA powders (MW=200000) were purchased from Jinan Daigang Biomaterial Co., Ltd. (Shandong, China). All reagents used in this experiment were of analytical grade and not further purified unless otherwise stated.

Preparation of PLLA/BT2 Piezocomposites: BT2 NRs were synthesized using a molten salt method and then subjected to surface modification with the silane coupling agent KH-560. To prepare the composite films, 0.5 g of PLLA powder was dissolved in 5 ml of DXA with vigorous magnetic stirring at 60 °C in a water bath for 6 h. Following this, varying amounts of surface-modified BT2 NRs (0, 5, 10, 15, 20, 25 wt.%) were added, and the mixture underwent alternating cycles of magnetic stirring and ultrasonication for 30 min each, repeated three times to obtain the precursor solution. This precursor solution was then cast onto clean glass substrates and coated uniformly to a thickness of 0.5 mm using a scraper-type automatic film coater. The glass substrates bearing the PLLA/BT2 liquid film were transferred to freezing at -75 °C for 8 h before being transferred to the vacuum chamber of a freeze-drying device, where they were vacuumed to induce solvent sublimation for 24 h. Once complete solvent removal was achieved, the resultant PLLA/BT2 composite film was carefully peeled off from the glass substrate. Subsequently, the obtained composite films were annealed in an oven at 110 °C for 1 h. For ease of description, these films were designated as PLLA/BT2- x , where x represents the content of BT2 NRs.

Fabrication of PLLA/BT2 PEHs: The prepared porous PLLA/BT2 composite film was precisely cut into square pieces measuring 3 cm \times 3 cm (with an effective working area of 2 cm \times 2 cm). Flexible conductive copper electrodes were affixed to both sides of the samples. Subsequently, the samples underwent corona polarization at 60 °C and 8000 V for a duration of 1 h. Upon completion of the polarization process, wires were

led out from both electrodes, and the samples were encapsulated with polyimide tape for protection.

Characterization of materials and piezoelectric energy harvesters: XRD scattering patterns for BT2 NRs and PLLA/BT2-*x* were characterized by X-ray diffraction (XRD, 7000, Shimadzu, Japan). Raman spectroscopy of BT2 NRs was tested by Raman spectrometer (Alpha300R, WITec, Germany). TEM images of BT2 NRs were captured by field emission high-resolution transmission electron microscope (FE-TEM; Talos F200X, FEI, USA). The microscopic morphology of all samples was observed by field emission scanning electron microscope (FE-SEM, Clara GMH, Tescan, Czech Republic). Distribution of elements in porous composite films were characterized using energy-dispersive X-ray spectroscopy (EDS). Fourier transform infrared spectroscopy (FTIR, TENSOR27, Bruker, Germany) was used to further analyze the phase structure of PLLA. Differential scanning calorimetry (DSC, DSC 214 Polyma, NETZSCH, Germany) was used to determine the melting point of PLLA and calculate its crystallinity. Precision impedance analyzer (DMS2000, Partulab, China) was used to analyze the dielectric constant and loss of PLLA/BT2-*x*. The tensile properties of PLLA/BT2-*x* were measured by universal testing machine (3344, Instron, USA). Oscilloscope (DS102E, RIGOL, China) and electrochemical workstation (CHI660E, CH Instruments, China) were used to measure the piezoelectric signal output by PLLA/BT2-*x* PEH. The Zeta potential of piezocomposite films was measured by Zeta potential analyzer (DT-330, DTI, USA).

Animals: Male C57BL/6 wild-type mice (6-8 weeks old) were purchased from the experimental animal center of the Fourth Military Medical University (Xi'an, China). All mice were housed in a specific-pathogen-free environment with a 12-h light/dark cycle at temperature (24±1°C) and relative humidity (50±5%), allowed free access to food and water. This study was approved by the Fourth Military Medical University Committee on Animal Care (IACUC-20240561). All experiments were performed according to the National Institutes of Health Guidelines on the Use of Laboratory Animals.

Micro-CT: Mice femoral were dissected free of soft tissue, fixed overnight in 10% formalin at 4°C for 48 hours and scanned at 65 kV, 153 mA, and a resolution of 8- μ m using the micro-CT (Skyscan 1172, Bruker). NRecon and CTAn software (Bruker) was used for reconstruction and quantification. Briefly, we selected the regions of interest to perform 3-dimensional histomorphometry analysis of trabecular bone, determining trabecular BV/TV, Tb.Th, Tb.N and Tb.Sp.

Histological analysis: After dissected free of soft tissue and fixed overnight in 10% formalin for 48 hours, mice femoral were placed in 0.5M EDTA (Servicebio, China) decalcification for 3 weeks (replaced once every three days) and embedded in paraffin, sliced into 10 μ m thickness, and stained with H&E and Safranin O-Fast Green staining following the standard protocol. Images were visualized using panoramic scanner (PanoView, China).

Antibacterial Performance of PLLA/BT2 piezocomposites films: Antibacterial analysis of various membranes was carried out using the incubation of *Staphylococcus aureus* (*S. aureus*, ATCC25923). Circular membrane patches ($d = 10$ mm) were placed in 48-well culture plates after being exposed to ultraviolet light for 4 h, then 100 μ L *S. aureus* suspension (1×10^5 CFU/mL) was added into each well and the incubation was continued for 24 h at 37 °C. To quantitatively evaluate the live and death of *S. aureus* after contacting various membranes, 10 μ L liquid was drawn from each well and evenly smeared in solid agar Luria Bertain (LB) plate, and cultivated for another 24 h at 37 °C. Then colonies on the LB plates were photographed under an optical microscope (Nikon, Japan).

Cell Proliferation Assay: For cell proliferation experiments, mc-3T3 (3×10^3 cells/well) were seeded onto different sterilized membranes ($d = 5$ mm) in 96-well plates and cultured with α -MEM containing 10% FBS and 1% Penicillin/Streptomycin (P/S). After 1, 3, 5, and 7 days of cell growth, 10 μ L CCK-8 solution (Beyotime, China) was added into each well of the different groups and incubated for 4 h at 37 °C. Cell proliferation was then assessed by measuring the absorbance at 450 nm using a microplate reader (Tecan, Switzerland). In parallel, live/dead assay were observed by fluorescent staining and images were captured using fluorescence microscope (Zeiss,

German). For live/dead assay, mc-3T3 (1×10^5) were seeded onto different sterilized membranes ($d = 15$ mm) in 12-well plates. After 7 days of culture, a calcein-AM/PI double staining kit (Solarbio, China) was applied.

Statistical Analysis: Data were presented as means \pm standard deviation (SD). For comparisons involving multiple groups, one-way ANOVA analysis was followed by Tukey's post-hoc test for normally distributed data. All statistical analyses were performed using GraphPad Prism v.9.4 software. P values < 0.05 were considered statistically significant.

Ethical Statement: All participating subjects were co-authors of this manuscript and informed, written consent of all participants was obtained before participation in the study.

1. Calculation of PLLA crystallinity (χ_c):

$$\chi_c = \frac{\Delta H_f}{\Delta H_f^0 \times \left(\frac{1}{1+wt.\% filler}\right)} \times 100\% \quad (\text{Equation S1})$$

Where ΔH_f represents the enthalpy of fusion measured, ΔH_f^0 (93.3 J/g) is the standard melting enthalpy of PLLA, and *wt.% filler* represents the mass ratio of BT2 NRs and PLLA.

2. Calculation of power density (P) of PLLA/BT2 PEH:

$$P = \frac{V_{OP}^2}{RS} \quad (\text{Equation S2})$$

Where V_{OP} , R and S represents the output voltage, external resistance and effective working area, respectively.

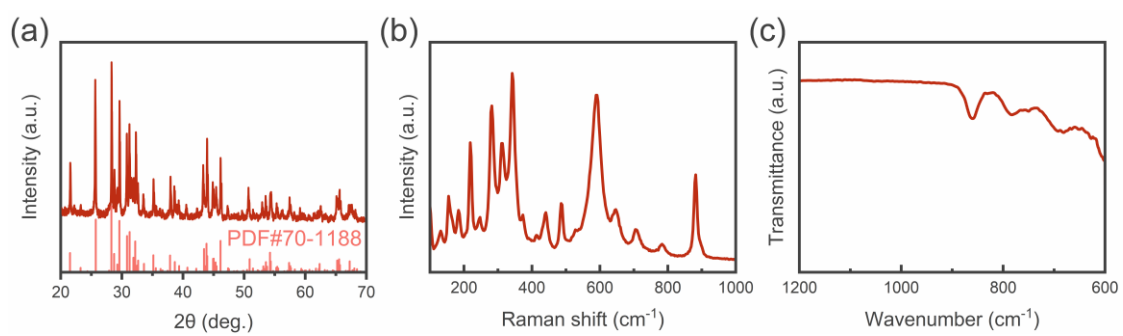


Figure S1. (a) XRD scattering pattern, (b) Raman spectra and (c) FTIR spectra of BT2 NRs.

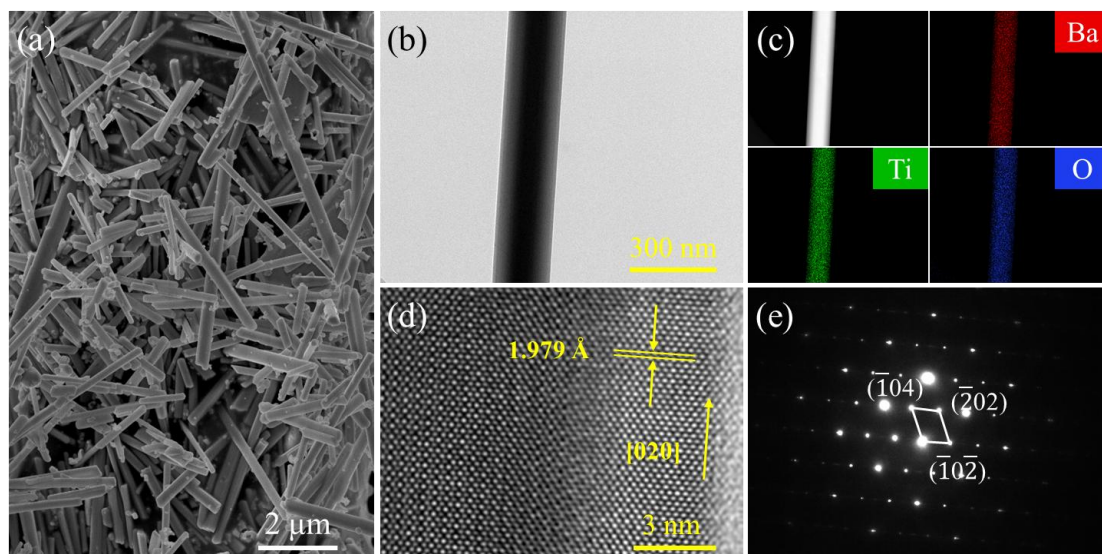


Figure S2. (a) SEM, (b) TEM, (c) EDS mapping, (d) HRTEM and (e) SAED images of BT2 NRs.

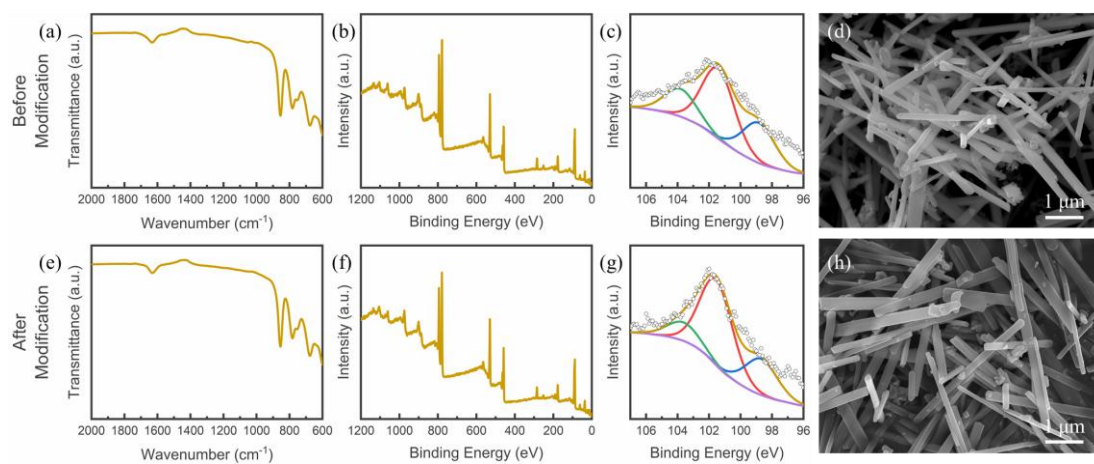


Figure S3. FTIR, XPS full spectra, fine spectra of Si and SEM images of BT2 NRs (a-d) before modification and (e-h) after modification.

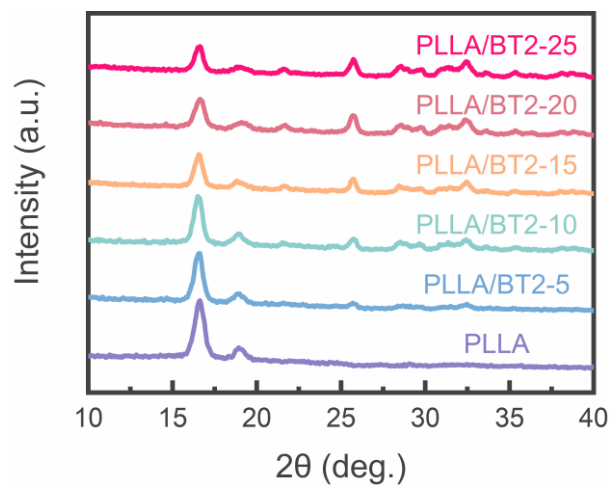


Figure S4. XRD patterns of PLLA/BT2-*x*.

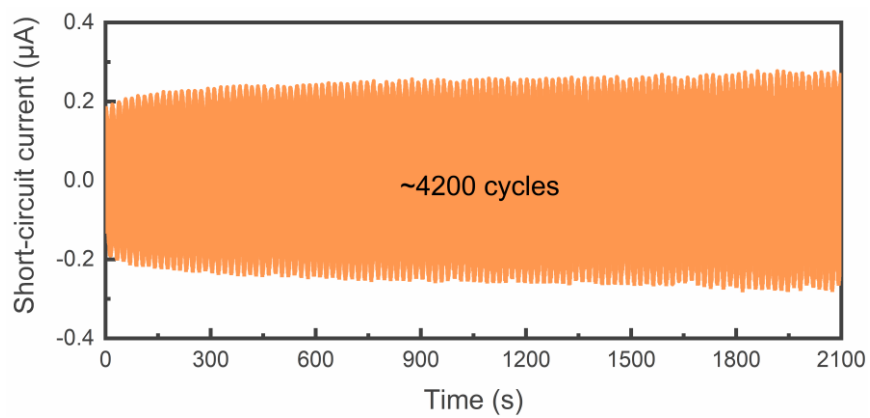


Figure S5. The stability and durability test results of PLLA/BT2-15 PEH.

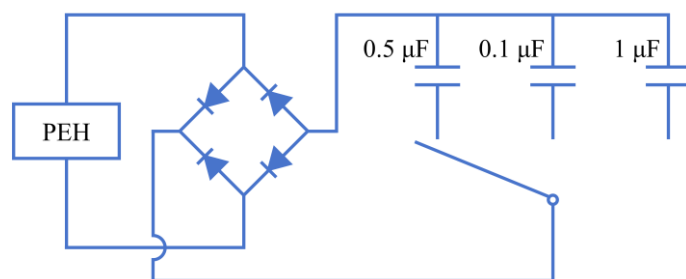


Figure S6. Schematic diagram of the circuit for charging the capacitor using PLLA/BT2-15 PEH.

No.	1	2	3	4	5	Average
Zeta Potential [mV]	0.25	0.17	0.13	0.21	0.24	0.2

Table S1. Zeta potential of the PLLA/BT2-15 composite (2 cm × 1 cm) measured in aqueous environment at pH 3.7 and room temperature.

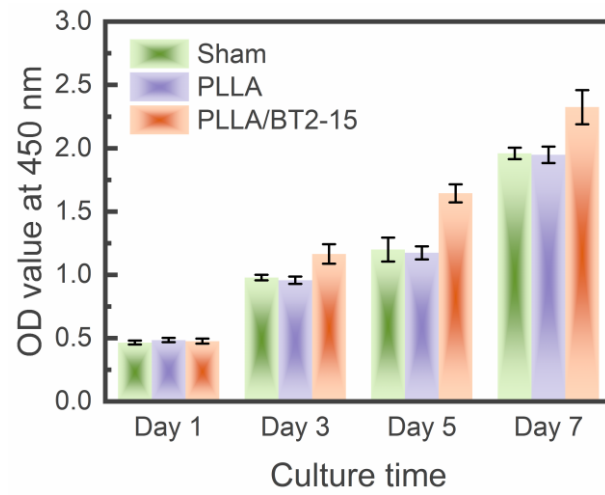


Figure S7. Proliferation rate of BMSCs within 7 days of (a) Sham, (b) PLLA and (c) PLLA/BT2-15 intervention.

Table S2. Comparison of the output performance and the energy conversion efficiency between the PLLA/BT2 PEH with other piezoelectric energy harvesters.

Materials	Filler's shape	Method	Structure	V_{OC} [V]	I_{SC} [μ A]	Power	Ref.
						density [μ W cm ⁻²]	
PLLA/K _{0.5} Na _{0.5} NbO ₃ @PDA	Nanowires	Electrospinning	Fibrous	17.9	2.6	/	[1]
PVDF/CaTiO ₃	Nanoparticles	Casting	Dense	20	0.25	0.19	[2]
PDMS/Bi ₄ Ti ₃ O ₁₂	Nanoparticles	Spin coating	Dense	12.5	0.1	562	[3]
PDMS/BaTiO ₃ @C	Nanoparticles	Casting	Dense	31	1.8	45.4	[4]
PVDF/ZnSnO ₃ @Ag	Nanocubes	Casting	Dense	20	/	/	[5]
PVDF-TrFE/BaTiO ₃ @PMMA	Nanowires	Electrospinning	Fibrous	12.6	1.3	0.68	[6]
PVDF-TrFE/BaTiO ₃	Single-crystal	Hot pressing	Dense	15.1	2.39	17.33	[7]
PDMS/(Ba _{0.85} Ca _{0.15})(Ti _{0.9} Zr _{0.1})O ₃	Porous pillars	Freeze casting	Dense	30.2	13.8	96.2	[8]
PVDF/BaTi ₂ O ₅	Nanorods	Electrospinning	Fibrous	31.2	0.52	2.46	[9]
PLLA/BaTi ₂ O ₅	Nanorods	TIPS	Porous	49.0	4.2	15.6	This work

References

1. P. Chen, C. Xu, P. Wu, K. Liu, F. Chen, Y. Chen, H. Dai and Z. Luo, *ACS Nano*, 2022, **16**, 16513-16528.
2. S. Panda, S. Hajra, H. Jeong, B. K. Panigrahi, P. Pakawanit, D. Dubal, S. K. Hong and H. J. Kim, *Nano Energy*, 2022, **102**, 107682.
3. N. P. M. J. Raj, N. R. Alluri, G. Khandelwal and S. J. Kim, *Composites, Part B*, 2019, **161**, 608-616.
4. Z. Zhou, X. X. Du, Z. Zhang, J. K. Luo, S. Y. Niu, D. Shen, Y. Y. Wang, H. Yang, Q. L. Zhang and S. R. Dong, *Nano Energy*, 2021, **82**, 105709.
5. A. Sasmal, A. Patra, P. S. Devi and S. Sen, *Compos. Sci. Technol.*, 2021, **213**, 108916.

6. K. Shi, B. Chai, H. Zou, P. Shen, B. Sun, P. Jiang, Z. Shi and X. Huang, *Nano Energy*, 2021, **80**, 105515.
7. R. Peng, B. Zhang, G. Dong, Y. Wang, G. Yang, J. Zhang, B. Peng, Y. Zhao and M. Liu, *Adv. Funct. Mater.*, 2024, **34**, 2316519.
8. M. Y. Yan, J. W. Zhong, S. W. Liu, Z. D. Xiao, X. Yuan, D. Zhai, K. C. Zhou, Z. Y. Li, D. Zhang, C. Bowen and Y. Zhang, *Nano Energy*, 2021, **88**, 106278.
9. Z. Shao, X. Zhang, J. Liu, X. Liu and C. Zhang, *Small Methods*, 2023, **7**, 2300701.